TUTORIAL REVIEW

CSR
www.rsc.org/csr

Excitement in f block : structure, dynamics and function of nine-coordinate chiral lanthanide complexes in aqueous media†

David Parker
Department of Chemistry, University of Durham, South Road, Durham, UK DH1 3LE.
E-mail: david.parker@durham.ac.uk; Fax: +44 (0)191 384 4737; Tel: +44 (0)191 3342033

Received 29th October 2003
First published as an Advance Article on the web 13th February 2004

Lanthanide complexation chemistry has been studied intensively over the past 15 years and progress has been stimulated by the advent of well-defined, kinetically robust systems tailored to applications as bioactive probes for magnetic resonance and luminescence. In this *tutorial review*, the extent to which an enhanced understanding of the relationship between complex structure and spectral properties is emerging is discussed, together with an examination of the mechanism of ligand exchange processes. Such issues are aiding the development of responsive probes, ranging from simple sensors to more complex studies defining water structure and exchange dynamics.

1 Historical perspective

Thirty years ago, undergraduates taking a lecture course in lanthanide chemistry might have had good reason for being rather uninspired by the content of the lectures. Beyond their important spectral and magnetic properties, much of the chemistry discussed would relate to the ubiquity of the tripositive oxidation state, the efficiency of ion exchange chromatography or solvent extraction in devising separations of lanthanide ion mixtures and the origins and validity of the lanthanide contraction, the 'gadolinium break' and the Russell-Saunders coupling scheme. How things have changed! Not only is there a rich and important organometallic chemistry of low oxidation states and a worldwide activity in chemo- and stereoselective Lewis-acid catalysed processes, but also a rich and exciting solution coordination chemistry has been defined. An excellent compilation of reviews on lanthanide chemistry has just appeared[1] as well as a book highlighting the role of lanthanide coordination chemistry in biosystems.[2] In this short review, selected recent developments in aqueous lanthanide coordination chemistry are discussed, with an emphasis on the structure, dynamics and function of water-soluble, chiral lanthanide complexes.

David Parker was educated at the University of Oxford (BA 1978, D.Phil 1980), studying with John Brown, and in Strasbourg as a NATO Fellow with Jean-Marie Lehn. He returned to his native North-East in 1982, as a Lecturer at Durham University, has been a Professor since 1992 and is currently serving his second term as Head of Department. He has gained numerous prizes and awards, most recently being elected a Fellow of the Royal Society (2002). In the same year he received the Tilden Lectureship of the Royal Society of Chemistry, upon which this article is based. His research interests are diverse and currently embrace many aspects of the chemistry of chiral metal complexes in solution.

† Based on a 2003/4 Tilden Lectureship of the Royal Society of Chemistry first delivered in Strasbourg, 5th December 2003.

In tracing the development of this work, certain pioneering studies can be readily identified. Shift reagents in NMR were developed for spectral simplification and chiral analysis both in organic and aqueous media[3] but are much less frequently used nowadays because of the advent of high field, pulsed multi-dimensional NMR techniques. This work typically involved studies of formally hexacoordinated Ln(III) species with Lewis bases (Ln, = Eu, Yb, Pr) in which the anisotropic spatial distribution of unpaired f electrons gives rise to a dipolar lanthanide-induced-shift for the bound Lewis base in solution. This is often termed a pseudo-contact shift. In the Gd(III) ion, on the other hand, there is an isotropic distribution of the f^7 electrons so that no NMR dipolar shift is produced. However, when a ligand binds to the paramagnetic Gd(III) centre, both the rates of longitudinal (R_1) and transverse (R_2) relaxation are enhanced considerably, giving rise to extensive line-broadening in the NMR spectra of bound ligand nuclei. In an early example of the use of the aqua Gd(III) ion as a relaxation agent, the line-broadening induced by a Gd^{3+}/lysozyme complex in the proton NMR resonances of the inhibitor, β-methyl-*N*-acetylglucosamine, was analysed in terms of the distances between the sugar protons and the paramagnetic ion.[4] Such work stimulated a great deal of activity on the application of the aqua lanthanide ions as shift and relaxation probes for NMR,[5] culminating in the development of both gadolinium contrast agents for clinical[6] MRI and the exploration of various shift reagents for magnetic resonance spectroscopy *in vivo* – for example, in real-time ^{31}P or ^{23}Na NMR analyses of perfused cells or intact animals using wide-bore magnets or surface-coil NMR probes. In addition, building on early work in Oxford[7] that established the importance of pseudocontact shift values as constraints in biomolecular structure determination, solution structures of proteins may now be determined with the aid of Ln^{3+} NMR probes[8] – often made more precise by the analysis of residual dipolar couplings and the introduction of cross-correlation and relaxation constraints.[5]

The lowest energy excited states of several of the lanthanide (III) ions have natural radiative lifetimes of the order of milliseconds, an attractive feature for a luminescent probe as it allows time-resolved detection procedures to be used, affording excellent discrimination between probe emission and background fluorescence or light scattering. Early work centred on the use of Eu and Tb aqua ions as probes for proteins and nucleic acids.[9] For example, binding of the Tb^{3+} aqua ion to single-stranded nucleic acids is characterised by an enhanced terbium emission intensity, which is not observed for doubly-stranded systems. Many studies involved the replacement of Ca^{2+} in a protein by a Ln^{3+} ion of similar size and charge density, for example in the Ca-binding proteins calmodulin, calbindin and parvalbumin.[10] The proximity of the Ln^{3+} ion through space to Trp

DOI: 10.1039/b311001j

or Tyr residues in the protein could be studied because the energy transfer process *e.g.* Trp→Tb, that leads to sensitisation of Ln emission, may be interpreted in terms of a dipole–dipole interaction and follows an r^{-6} dependence (*cf.* the r^{-3} dependence for pseudo-contact shifts in NMR).

With the more recent discovery of well-defined series of water-soluble, kinetically stable, chiral lanthanide complexes differing in overall charge, hydrophilicity (numbers of H-bond donors and acceptors) and denticity,[11,12] there is an opportunity to make more effective use of Ln^{3+} probes in NMR and optical analyses of biomolecules. Examples of such structures are revealed in Scheme 1, together with an indication of their function. This review will focus on understanding the structural features of such systems and their reactivity and exchange dynamics that render them suitable for such applications. Key issues to address include: the determinants of ligand exchange at the Ln^{3+} centre; the structural factors controlling the magnitude of the dipolar NMR shift; the relationship between the coordination environment at the Ln^{3+} centre and the form, intensity and lifetime of optical emission spectra.

2 Structural analysis of aqua complexes

Ligand field splittings involving Ln^{3+} ground and excited states are typically much less than kT (*i.e.* < 200 cm^{-1} or 2.5 kJ mol^{-1}), so that an electrostatic model is a reasonable approximation in understanding their bonding and coordination preferences. Given the absence of any directional preference for the spherical, charge dense Ln^{3+} ion, it is expected that steric and ligand geometric constraints will be of prime importance in defining the preferred coordination number and geometry at the Ln^{3+} centre. Here, we consider a series of aqua complexes with coordination number 9, as typical examples, examining cases where the number of bound waters is either 9 or 1.

2.1 The Ln(III) aqua ions: $[Ln(OH_2)_9](CF_3SO_3)_3$

For the series of nona-aqua ions that crystallise with triflate counterions in the space group $P6_3/m$, there are two independent M–OH_2 distances. One defines the distance to the six vertices of a trigonal prism and the other characterises the longer distance to the 3 capping sites. Across the Ln series, the variation of the shorter Ln–OH_2 distance to the 6 vertices faithfully follows the ionic radius change, whereas for the longer bond to each capping position, the normalised distance lengthens by 0.06 Å for Lu compared to Ce. Such a variation reflects the ease of packing the 9 water molecules about the spherical ion, with the 3 capping bonds being elongated for the smaller ions as a result of the minimisation of steric repulsion between adjacent water molecules, Fig. 1.

2.2 Mono-aqua complexes

The isostructural series of complexes $[LnL^1(OH_2)](CF_3SO_3)_3{\cdot}3H_2O$ has been recently characterised crystallographically, in the space group $P2_1$, with the axial water molecule capping a regular square-antiprismatic coordination geometry, Fig. 2.[12] The bound water molecule acts as a H-bond donor to 2 triflate anions and as a H-bond acceptor to the nearest water molecule. Plots of the variation of Ln–ligand and Ln–OH_2 distances across the series revealed the same features observed with the nona-aqua ions and with the anionic complex $[LnL^2(OH_2)]{\cdot}4H_2O$: ligand O and N to Ln distances echo the ionic radius variation whilst the 'normalised' Ln–OH_2 distance is elongated by 0.05 Å (Pr→Lu), reflecting the steric compression induced as the Ln ionic radius diminishes, Fig. 3. A related example has been described by Mazzanti for some tripodal picolinate lanthanide complexes possessing two bound waters.[12] Thus, the capping water molecule occupies a sterically demanding position in each of these structurally diverse series of complexes. The longer the Ln–OH_2 bond, the more effective it should be as a H-bond acceptor leading to an enhanced H-bonding interaction with a water proton of an adjacent molecule. Across the

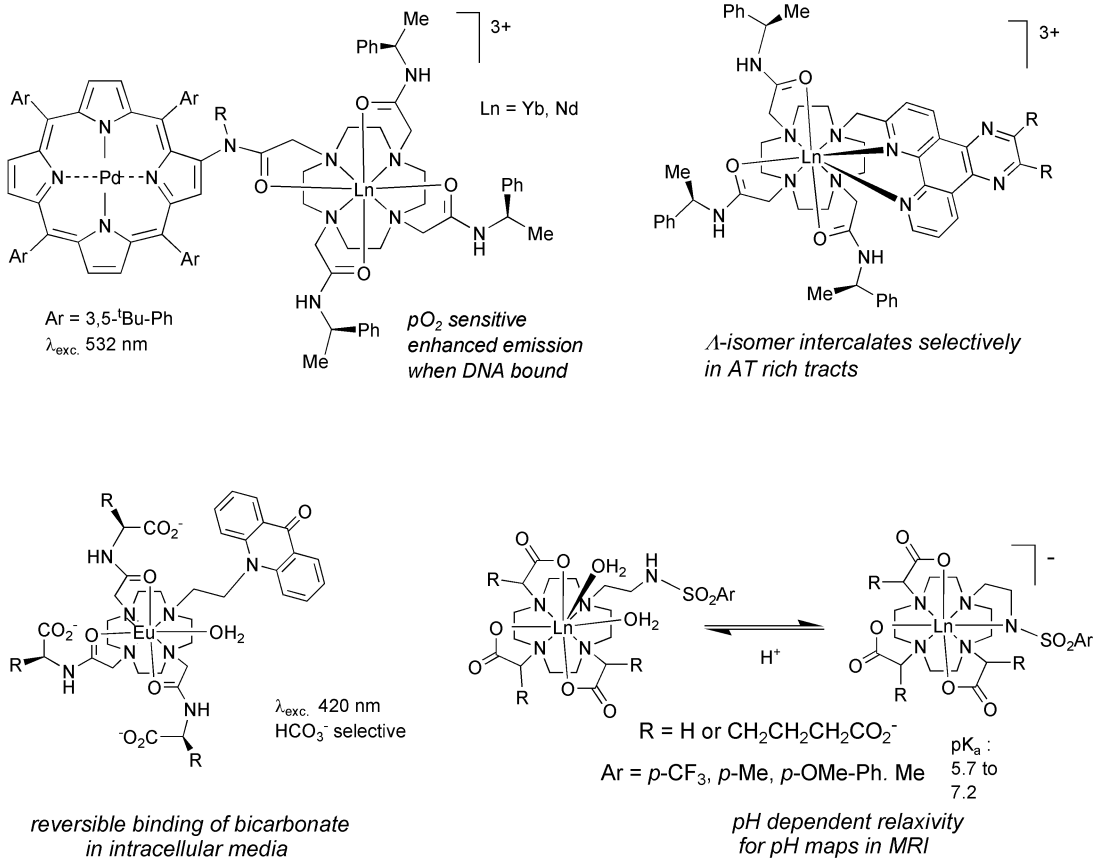

Scheme 1

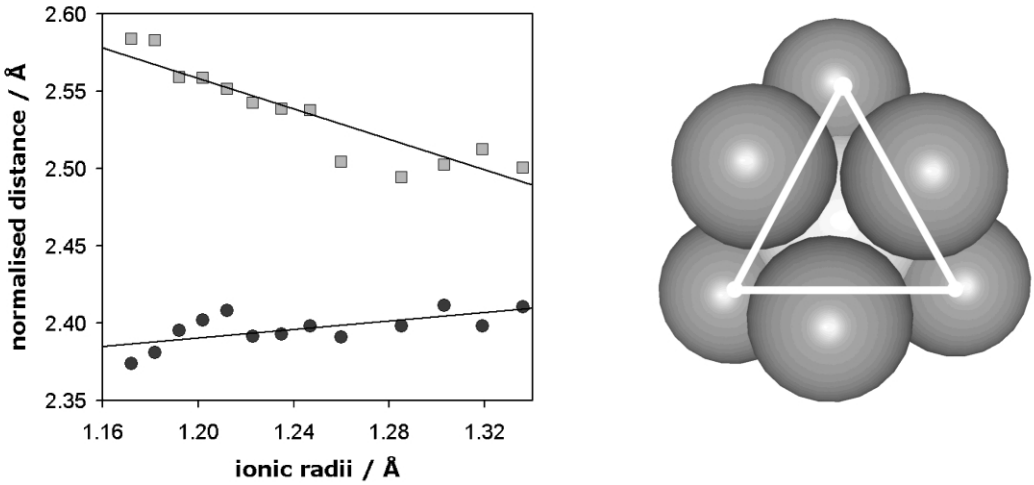

Fig. 1 Variation of the distance between the Ln ion (normalised to Gd) and the apical (circles) and capping (squares) waters in $[Ln(H_2O)_9](CF_3SO_3)_3$, showing the lengthening of the capping Ln–OH_2 bond distances across the series.

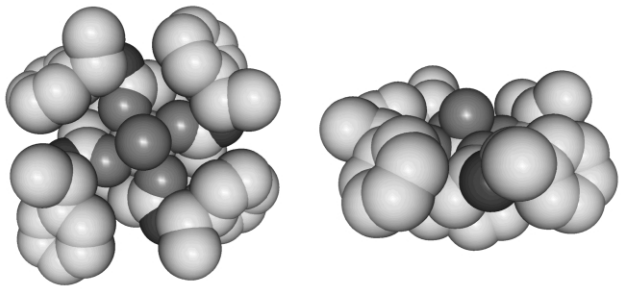

Fig. 2 End and side elevation showing the exposed axial water module in $[EuL^1(OH_2)](CF_3SO_3)(H_2O)_3$ occupying a sterically demanding site.

series, in $[LnL^1(OH_2)](CF_3SO_3)_3{\cdot}3H_2O$, whilst the distance between the bound water oxygen (H-bond donor ability) and the triflate oxygen does not change, the distance between the primary and second-sphere water oxygen decreases from 3.17 Å (Pr) to 3.04 Å (Lu), Fig. 4.[13]

These simple structural features are of interest in developing a better understanding of the transition state structure for water interchange – which occurs *via* a predominantly dissociative mechanism in this type of complex, as revealed in pioneering work from Merbach's group.[6] Features destabilising the ground state structure or stabilising the putative transition state structure – with respect to the water interchange reaction coordinate – should lead to rate enhancements for the water exchange process. The structural studies can only relate to the relative importance of ground state destabilisation, and will be of significance if the water exchange transition state structure resembles the ground state structure. Measurements of the rate of water exchange ($^1H/^{17}O$ NMR as a f(*T*/*P*)) show that in $[LnL^1]^{3+}$ and related cationic complexes of tetra-amide ligands,,[14,15] the central ions (Eu, Gd, Tb) exchange water most slowly, while the later ions (Tm, Yb) exchange more than one hundred times faster. Given the large positive entropies and volumes of activation that also typify water exchange in such cationic Eu, Gd, Tb complexes that adopt the regular square antiprismatic geometry,[6] it seems reasonable to assume that a significant part of the rate enhancement with the later smaller ions can be attributed to a process with an 'early' transition state structure, resembling the ground state. Of course, it is very likely that there is a very significant and favourable entropy term to consider, associated with the release of ordered counter-ions and water molecules from the second hydration sphere to bulk.

3 Determinants of water exchange rates: pre-eminence of the second sphere of hydration

A major driving force in seeking to improve our understanding of water exchange mechanisms has been the direct relationship to the improvement in the performance of Gd MRI contrast agents.[6,12,16] The mono-aqua anionic complexes of gadolinium *e.g.* $[Gd L^2(OH_2)]^-$ [or Dotarem, Guerbet s.a., Paris], are used routinely in thousands of MRI scans each year given at dose of 2 or 3 g per patient. They function by catalysing the rate of relaxation of the

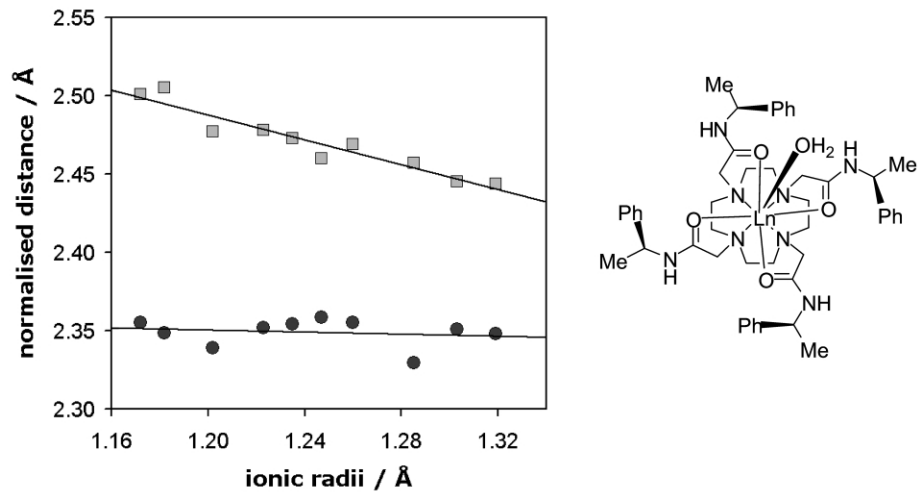

Fig. 3 Variation of the distance between the Ln ion (normalised to Gd) and the apical (circles) and capping (squares) waters in the isostructural series $[LnL^1(OH_2)](CF_3SO_3)_3{\cdot}H_2O_3$.

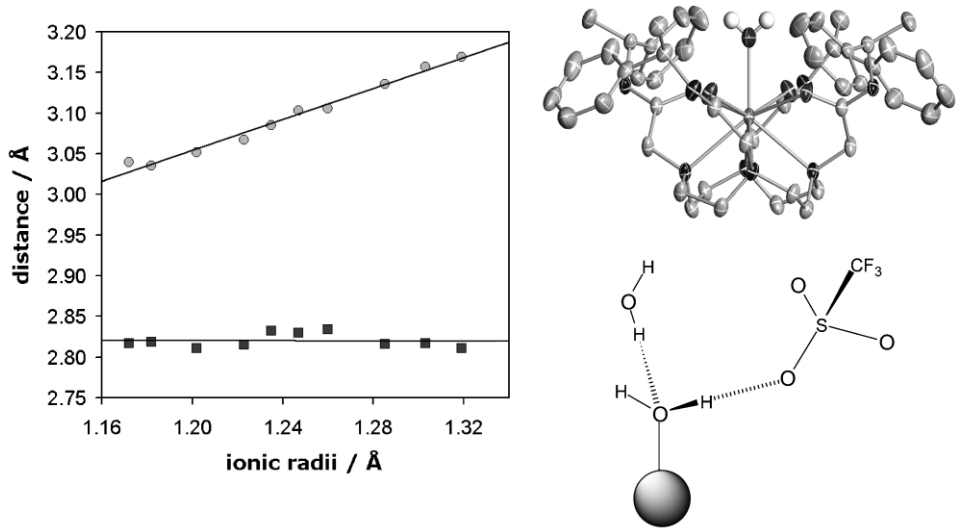

Fig. 4 Variation of the O–O distance across the Ln series in $[LnL^1(OH_2)](CF_3SO_3)_3(H_2O)_3$ between the bound water, acting as a donor to the triflate anion, and as a H-bond acceptor to the second sphere water (circles).

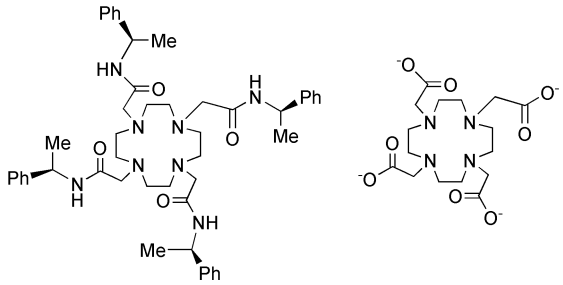

(RRRR)-L^1

L^2

bulk water protons. A useful parameter used to compare the efficacy of different gadolinium complexes is the *relaxivity* of a given complex. This is defined as the change in the water proton relaxation rate per unit concentration of added complex, and has the units $mM^{-1}\ s^{-1}$, *i.e.* those of a second order rate constant. The efficiency of this process can be limited by the rate of water exchange at the Gd centre, so that a great deal of research has focused on defining the key determinants of the water interchange mechanism and their relative importance. Over the past five years or so, a particular emphasis has been placed on assessing the nature of the second sphere of hydration, and factors influencing its structure and composition.[12,17]

3.1 Effect of complex geometry and isomerism

For the C_4-symmetric lanthanide complexes of L^2, L^3 and the tetra(carboxyethyl) analogue L^4 four isomeric species exist in solution, defined by their NCCO (Δ/Λ) and NCCN (δ/λ) torsion angles. Thus, in $[GdL^2(OH_2)]^-$, two chiral diastereoisomers exist: (Δ/λλλλ) sometimes loosely termed an 'M' (or SAP) isomer and adopting a regular square antiprismatic coordination with an N_4/O_4 twist angle of 40°, and (Λ/λλλλ), termed an 'm' (or TSAP) isomer with a 29° twist angle. Interconversion between these isomers may occur by cooperative arm rotation (Δ→Λ) or ring inversion (δ→λ). The latter process is generally rather slow in each complex (*ca.* 50 s^{-1} at 298 K), whilst the former is fast on the NMR timescale for $[LnL^2]$ but is frozen in the C-substituted complexes of L^3 and L^4.[18] In $[EuL^4(OH_2)]^{5-}$, the position of the equilibrium (SAP/TSAP) has been studied by VT and VP emission spectroscopy, showing the SAP isomer to be the more compact structure with a lower overall hydration state.[19] Detailed luminescence measurements of the apparent solution hydration state of the Eu and Tb complexes of L^3 and L^4, suggested that the bound water in the TSAP (m) isomer was longer than in the SAP complex.[18,20] Such an idea is consistent with the general observation from crystallographic studies that the Ln–OH_2 bond distance is longer for such TSAP (*cf.* SAP) complexes.[12] Indeed, in a recent analysis of the TSAP (m) complex $[TbL^5(OH_2)]^{2-}$ – the Tb–OH_2 bond length is 2.68 Å, which is 0.23 Å longer than in the SAP $[TbL^2(OH_2)]^-$ analogue. Furthermore, the distance between the bound oxygen and the second sphere water was only 2.78 Å. Such a structure can almost be considered as a snapshot of the developing transition structure for dissociative exchange, with the incoming water aiding release of the bound water through a strong H-bond interaction[21] . The exit pathway taken by the coordinated water appears to be linear, as even the longest measured lanthanide-water bond shows $< 3°$ deviation from linearity with respect to the principal coordination axis. Such behaviour is in accord with the long range r^{-1} dependence defining the electrostatic interaction between the charged lanthanide centre and the water oxygen.

Variable temperature ^{17}O-NMR studies have been used to measure the water exchange rates in the series of Gd complexes of L^2–L^4, including further stereoisomers of L^4, for which the SAP/TSAP molar ratio has been independently assessed. The data reveal

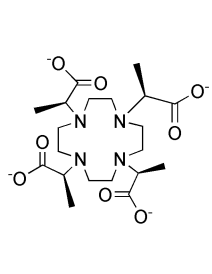

(SSSS)-L^3

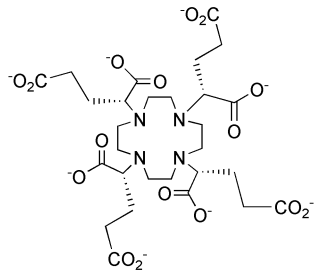

(RRRR)- L^4

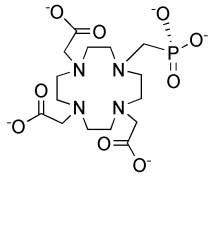

L^5

(Table 1), that the rate of water exchange is directly proportional to the mole fraction of the TSAP (m) isomer, and to a first approximation is at least 50 times faster for this species. Such a conclusion also accords with the hypothesis (section 2) that the bound axial water molecule is in a sterically demanding position, consistent with the lengthening of the Ln–OH_2 bond in the faster exchanging TSAP complexes.

Table 1 Water exchange rates (±10%) in related anionic Gd complexes (298 K, pH 6, ^{17}O-NMR analysis) as a function of isomeric composition[a]

Complex[b]	n_{TSAP}	K_{ex}^{obs}	K_{TSAP}^{calc} ($\times 10^7 s^{-1}$) (±0.2)
$[GdL^2(OH_2)]^-$	0.17	0.41	2.4
(SSSS)-$[GdL^3(OH_2)]^-$	0.70	1.47	2.1
(RRRR)-$[GdL^4(OH_2)]^{5-}$	0.70	1.54	2.2
(RRRS)-$[GdL^{4\prime}(OH_2)]^{5-}$	0.43	0.91	2.1
(RSRS)-$[GdL^{4\prime}(OH_2)]^{5-}$	0.17	0.34	2.0

[a] n_{TSAP} is the estimated mole fraction of the TSAP complex in solution, from NMR analysis of related Eu/Tb complexes. [b] The (*RRRS*), (*RSRS*)-isomers of L^4 are denoted $L^{4\prime}$.

3.2 Effect of ligand hydrophobicity

The extent and structure of the second sphere of hydration that surrounds these lanthanide complexes is a sensitive function of the nature and relative position of ligand substituents. In a detailed analysis of the degree of hydration of the Eu, Gd and Tb complexes of L^6 and L^7, existing as one preferred TSAP complex in solution, using VT ^{17}O-NMR, water proton relaxation rate and luminescence kinetic studies, it was evident that each complex possessed no inner sphere water molecule. However the [EuL^7] complexes apparently gave fractional hydration states (typically 0.5) by luminescence analysis. These values correlated very well with the enhanced relaxivities of the Gd analogues and the variation in the estimated distance between the Gd ion and the water proton.[20,22] In the luminescence method of determining hydration states, the loss of excited state energy from the Ln ion to vibrational energy of bound or proximate OH oscillators occurs *via* a Forster mechanism in which dipole–dipole interactions dominate. This follows an r^{-6} dependence (Ln ion to OH oscillator). Similarly, an r^{-6} dependence characterises the dependence of the water proton longitudinal relaxation ratio, R_1, on the water proton distance to the Gd ion. Thus the apparent hydration state, q', of such complexes is a sensitive function of the Ln–OH_2 distance, Fig. 5, when determined by luminescence or relaxometric studies. Indeed, a lengthening of a typical Ln–OH_2 bond by 0.2 Å results in an apparent hydration state of 0.68, and when a water molecule diffuses within 3.6 Å of the Ln ion, an apparent hydration state of 0.25 is found. This distance is a very reasonable value for a second sphere water molecule,[12,17] when compared to relevant crystallographic data.[12]

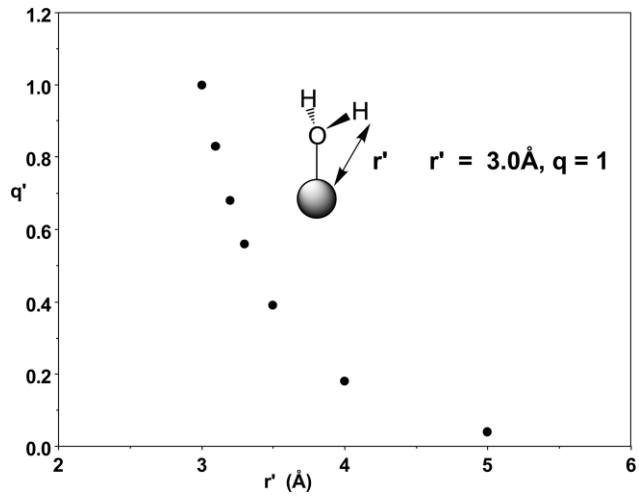

Fig. 5 Variation of the apparent hydration state q' ($0 < q' < 1$) with the distance between a proximate OH group and the Ln ion. The distance 3.0 Å is taken to represent $q' = 1$ and the r^{-6} dependence is assumed to characterise the distance dependence of vibronic quenching and paramagnetic proton relaxation.

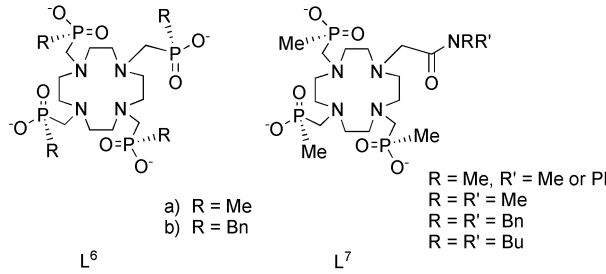

A striking example of the way in which the extent of second-sphere hydration can determine the rate of water exchange is provided by a series of cationic Eu tetra-amide complexes, Fig. 6.

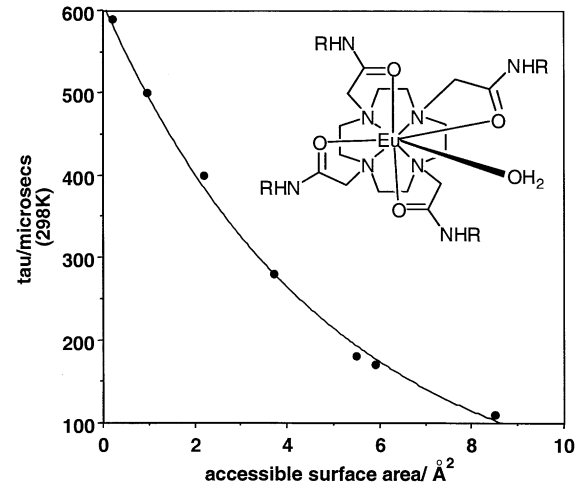

Fig. 6 Variation of the exchange lifetime (τ_m, μs, 298 K) for related series of europium tetraamide complexes, with the calculated solvent accessible surface area (Å^2).

The nature of the secondary amide substituent determines the extent of the accessible surface area available for water molecules to diffuse freely. This, in turn, restricts the rate of water exchange so that the exchange lifetime, ($\tau_m = k_{ex}^{-1}$), is longest for the complexes with the smallest solvent accessible surface area.[15] Such studies are of particular importance in the recent development of paramagnetic CEST contrast agents (Chemical Exchange by Saturation Transfer), for which maximisation of the water exchange lifetime is highly desirable.[23]

3.3 Effect of counterion

In Eigen, Wilkins' and Margerum's early work on the mechanism of ligand exchange at metal centres, the simple water exchange reaction was considered to be insensitive to the nature of the ligand in the second coordination sphere, *i.e.* independent of the unbound counter-ion, and was controlled by the rate of water association or dissociation.[24,25] However, it is apparent that the extent, structure and degree of order of the second sphere of hydration is a key determinant in defining the free energy of the transition state structure for water exchange. Moreover, given that the secondary hydration structure will be determined not only by the charge density of the metal ion involved (section 2.2), but also by the nature of the counterion, water exchange rates are expected to be dependent on both variables. Charge densities govern water/ion

interactions and define both the relative importance of ion–water dipole interactions and the extent of hydrogen bonding involving water–water hydrogen bonds. More charge dense ions impose strong electrostatic order, breaking hydrogen bonds and creating a well-defined and ordered second sphere of hydration.[26] Less charge dense ions (*e.g.* large or 'soft' anions) do not perturb the bulk water hydrogen bonding significantly and are sometimes termed chaotropes (*e.g.* $I^- > Br^- > Cl^-$) to distinguish them from what are sometimes termed kosmotropes (*e.g.* Ln^{3+}, Mg^{2+}, $Li^+ > Na^+ > K^+$; phosphate anions), which serve to enhance ionic and solvent ordering.[27]

A simple example of how the nature of the anion can determine the structure of the second hydration sphere is given by the series of complexes $[GdL^1(OH_2)](X)_3{\cdot}nH_2O$, each crystallised from water. Comparing triflate and nitrate complexes, for example, the hydrogen bonding array is quite different, Fig. 7, with 2 nitrate

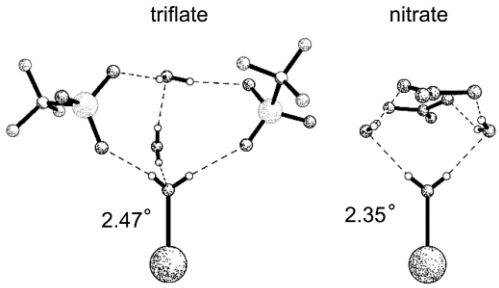

Fig. 7 Local hydrogen bond network in the cationic complexes of $[GdL^1](OH_2)\,(X)_3{\cdot}3H_2O$ for triflate and nitrate complexes.

anions capping the structure and forming H-bonds to two second sphere waters that also act as H-bond acceptors to the coordinated water. With a triflate anion, the coordinated water also acts as a H-bond donor and the Ln–OH_2 distance extends to 2.47 Å, compared to 2.35 Å in the nitrate! Crystal structures of the Cl^-, Br^- and I^- salts show an increasing degree of disorder, to such an extent that the location of the third Br^- or I^- anion and surrounding waters in the lattice cannot be determined by X-ray crystallography.

An illustration of the importance of the anion in determining water exchange kinetics is provided by the series of Gd complexes of L^8, varying the anion, and the related α and β-alanine derivatives L^9 and L^{10}. The rate of water exchange at the Gd centre is anion dependent[28] (k_{ex} follows the order $I^- > Br^- > OAc^- > CF_3CO_2^- \sim Cl^- \sim SO_4^{2-}$) and is also reflected in the lower proton relaxivity (relaxivity is the increment of the water proton relaxation rate per mmol of Gd complex) of the Gd complexes (Fig. 8). For the more slowly-exchanging complexes, the relaxivity tends to the limit predicted for a complex where only the outer-sphere contribution to the measured proton relaxivity is operative, *i.e.* under conditions when the water exchange rate is very slow.[28]

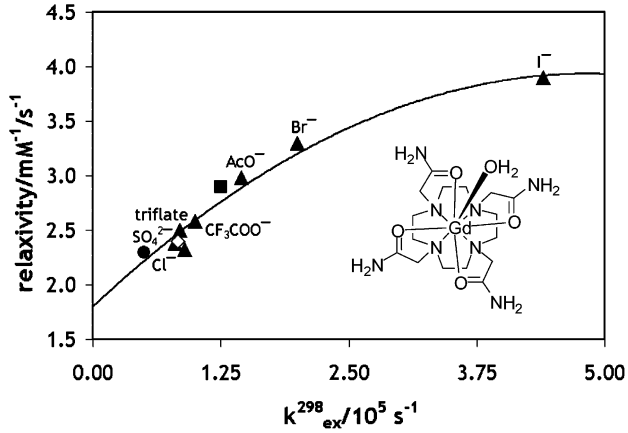

Fig. 8 Variation of water proton relaxivity (298 K, 20 MHz) with water exchange rate (^{17}O NMR) for the series of $[GdL^8(OH_2)](X)_3$ complexes changing the anion as shown. Data for complexes $[GdL^9(OH_2)]^{3-}$ (circle) and $[GdL^{10}(OH_2)]^-$ (square) are shown for comparison.

4 Emissive lanthanide complexes: correlating structure and NMR/optical spectral profiles

Much of the early work with emissive lanthanide complexes was driven by the desire to maximise the emission quantum yield using an integral chromophore (high ε) that attained the longest possible excitation wavelength, and hence favoured their use as luminescent tags or FRET components in biochemical analyses. Examples include the terbium complex, $[TbL^{11}]^{3+}$ (ϕ_{em} = 0.41, λ_{exc} 355 nm, H_2O, 298 K)[29] and various acridone conjugates of macrocyclic Eu complexes in which the excitation wavelength can be 410–420 nm.[30,31] A photophysical scheme that characterises the processes that follow light absorption by the sensitising chromophore, Scheme 2, highlights the requirements for high quantum yields of Ln emission for such conjugates.[11,32] The chromophore (Ar) should absorb light efficiently, and undergo efficient inter-system crossing to populate a triplet state that is $\geq 1700\ cm^{-1}$ higher in energy than the accepting state of the Ln^{3+} ion. Efficient intramolecular energy transfer then requires the minimisation of the distance between the Ln ion and the chromophore. The Ln excited state, once populated, must be shielded from deactivation by vibrational energy transfer to energy-matched XH oscillators,[20] *e.g.* by excluding coordinated water molecules. Any competitive processes that may quench the three excited states in this pathway (S_1, T_1 and Ln), such as charge transfer or collisional quenching, will also reduce the Ln emission quantum yield. However, the intermediacy of the three excited states affords an opportunity to modulate the intensity, polarisation, lifetime and spectral form characterising the final Ln emission. Indeed, lanthanide sensors based on modulation of singlet quenching (*e.g.* for Cl^-, Br^-; intensity only),[33] triplet quenching (*e.g.* for

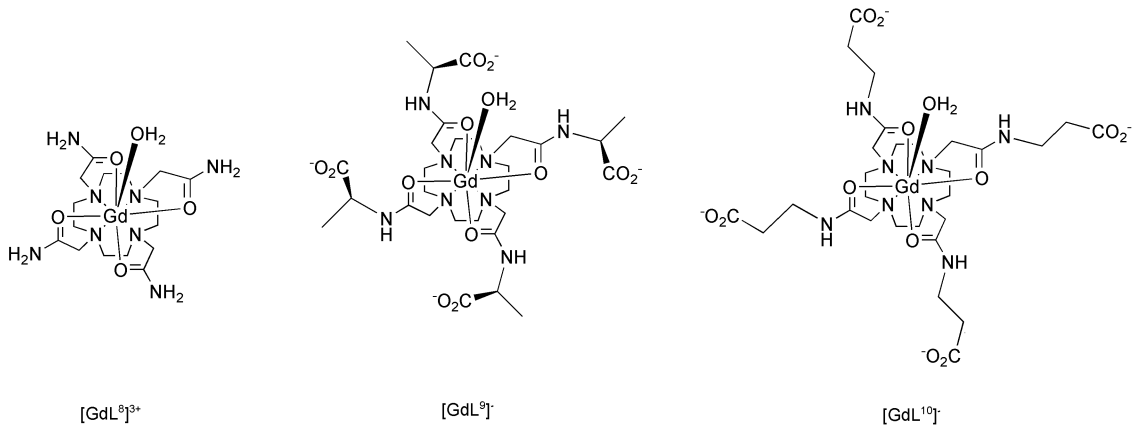

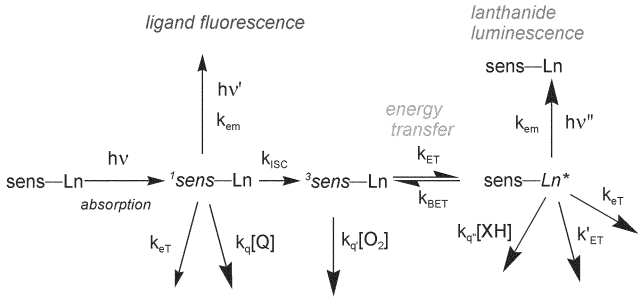

Scheme 2

O_2; lifetime/intensity)[34] and Ln deactivation (*e.g.* for anions displacing Ln bound waters) have been devised,[31,35,36] (see also section 5).

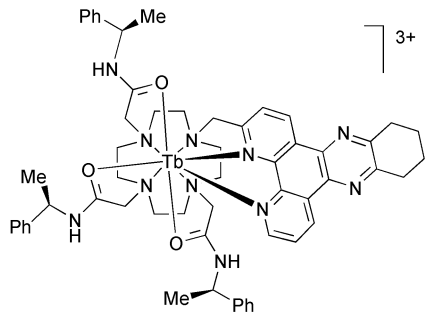

$[TbL^{11}]^{3+}$

Whilst it is generally accepted that the optical and NMR[37] spectral properties of the paramagnetic lanthanide complexes are determined by the nature and local symmetry of the coordination environment, there have been very few studies that seek to determine the relationship between donor atom charge, geometry and polarisability and the measured NMR dipolar shifts and optical emission spectra.[38,39] The link between the two can be found in Bleaney's theory of magnetic susceptibility anisotropy,[37] wherein a second-order ligand field coefficient is involved. The paramagnetic lanthanide induced shift is given as the sum of contact and pseudo-contact terms, eqn. (1), where C_j are 'Bleaney' factors characteristic of a given $4f^n$ configuration,

$$\delta^{para} = \langle S_z \rangle_j F_i + C_j B\, {}^2_0G_i = \delta^c_{ij} + \delta^{pc}_{ij} \qquad (1)$$

G_i is a geometrical term relating to the spherical polar coordinates of the given nucleus ($G_i \propto (3\cos^2\theta - 1)/r^3$), F_i is the contact term proportional to the hyperfine Fermi constant (A_i) and $\langle S_z \rangle$; is the spin expectation value of the S_z operator. In axial symmetry, a good approximation for the pseudocontact (dipolar) NMR shift is given by eqn. (2), where θ and r define polar coordinates with respect to the principal axis and $C_J = g^2J(J+1)(2J-1)(2J+3)\langle J/a/J^1 \rangle$. For Yb and to a lesser extent Eu, the pseudocontact shift δ^{pc} dominates the observed paramagnetic shift.

$$\delta^{pc}_{ij} = \frac{2C_j\beta^2}{(kT)^2}\frac{\left(3\cos^2\theta - 1\right)B_o^2}{r^3} \qquad (2)$$

Analysis of Eu optical emission spectra is the simplest to undertake amongst the emissive Ln ions because of the absence of degeneracy of the luminescent ^5D_o excited state. The relative intensity of the electric-dipole allowed $\Delta J = 2$ transition provides information on donor atom polarisability and in axial symmetry the splitting of the two allowed $^7F_1 \rightarrow {}^5D_o$ $\Delta J = 1$ transitions is directly proportional to B_0^2 (eqn. (2)). Using the C_4-symmetric complex, $[EuL^1(MeCN)]^{3+}$, as a model system, the axial donor may be systematically varied by displacement of the weakly bound acetonitrile molecule, (Fig. 9). An excellent correlation has been obtained between the measured NMR chemical shift of the most shifted ring CHN proton and the value of B_0^2, determined optically.[39] Furthermore, it is the polarisability of the axial donor in such complexes that ranks B_0^2 in an order which not only defines donor affinity to the charge dense Ln cation, *e.g.* HMPA > DMSO > DMF > H_2O/ROH > $MeNO_2$ > MeCN, but also determines the ratio of the intensities of the $\Delta J = 2/\Delta J = 1$ transitions.[39] With this knowledge and a related analysis for anionic donors,[41] it now becomes much easier to analyse comparative lanthanide induced paramagnetic NMR shift data, relate it to interpretation of Eu emission spectra and hence *deduce* direct information about the nature of the coordination environment at the Ln ion.

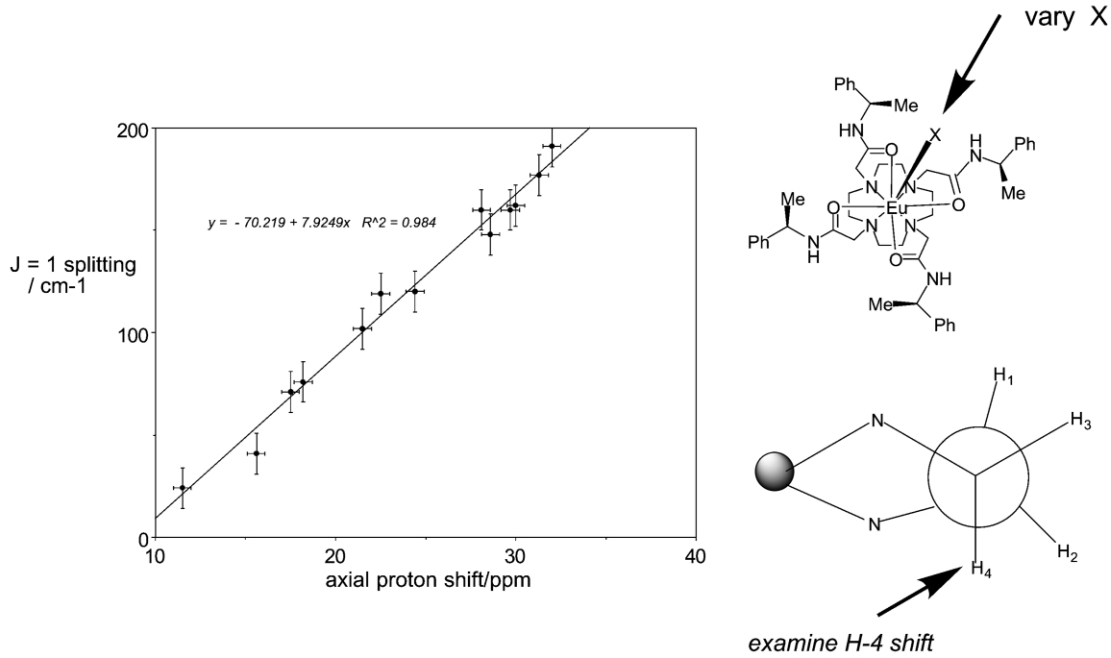

Fig. 9 Correlation of the axial proton NMR shift for the most shifted ring resonance H-4, with the measured separation of the two $\Delta J = 1$ bands in the optical emission spectrum (298 K, H_2O), vindicating Bleaney's theory of magnetic susceptibility anisotropy.

5 Functional systems: responsive lanthanide complexes

There are two general classes of lanthanide complex which are being examined currently as probes for their local environment. The first relates to the development of responsive (or 'smart') contrast agents in which the relaxivity of the gadolinium complex is a function of pH,[35] pM[39,40] (*e.g.* M = Ca, Zn) or pX. There remain some substantive issues to address before practicable images showing local pH or pM gradients *in vivo* can be undertaken routinely. Of particular note is the need to overcome the problem of assessing in parallel the local concentration of the 'responsive' Gd complex: this is needed to calibrate the image signal intensity enhancement. Current work has established that sequential administration of two structurally related complexes (one responsive, the other not *e.g.* GdL^{12} and GdL^{4}) can lead to the acquisition of difference images that reveal, for example, local pH maps. In $[GdL^{12}]$, the intramolecular ligation of a sulfonamide nitrogen is pH dependent, allowing the switching between a high relaxivity diaqua species (acidic environment) and a much lower relaxivity N-bound species (q = 0), (Fig. 10). Controlled modulation of the

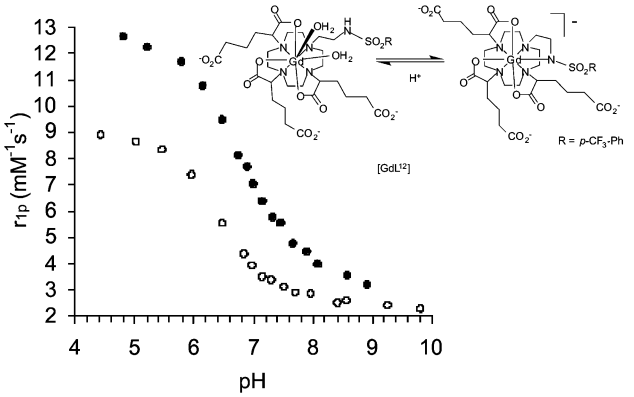

Fig. 10 Change in the relaxivity of $[GdL^{12}]$; (R = *p*-CF_3), as a function of pH in a simulated extracellular background (open circles) and in the presence of human serum albumin solution (298 K, 65.3 MHz).

operating pH range is achieved by variation of the sulfonamide substituent, and in one example a 48% increase in relaxivity between pH 7.4 and 6.8 was demonstrated.[35]

The second main class of complex is the responsive luminescent series,[31–36] discussed in Section 4. Most work to date has addressed the reversible displacement of one or both waters in diaqua complexes by anion ligation to the lanthanide centre.[36] This binding event is signalled by changes in the intensity and form of Ln emission, allowing ratiometric analyses to be undertaken. Such methods – averting the concentration dependence issue for the Gd systems discussed above – are most appropriate in analyses of Eu emission spectra. The relative intensity of the magnetic-dipole allowed ΔJ = 1 transitions (around 590 nm) is insensitive to the associated change in coordination environment whilst the intensity of the electric-dipole allowed ΔJ = 2 (616 nm) and ΔJ = 4 (around 702 nm) manifold changes considerably, particularly if the 'hard' axial water molecule is displaced by a more polarisable charged donor. An example of such emission spectra (Fig. 11) highlights the increase in the relative intensity of the ΔJ = 2 band (618 nm) for the carbonate-bound species – compared to lactate and citrate – and exemplifies how each bound anion gives a 'fingerprint' emission spectral profile, allowing simple identification and ratiometric analysis. This information is required in the application of such methods in complex media – where a large number of anions may compete in binding to the lanthanide centre. The structure of several of these ternary complexes has been defined by X-ray analyses (*e.g.* in chelated adducts with lactate, citrate, several amino-acids, acetate)[41] and by NMR studies on Eu and Yb analogues. Relative binding affinities have been assessed in simple competitive analyses or in fixed interference studies and reveal that in the millimolar range, it is the more polarisable (higher energy HOMO) oxygen in HCO_3^- (bound as CO_3^{2-}) and various phosphorylated di-anions which bind most avidly.

5.1 Hydrogencarbonate analysis: a promising case?

The bicarbonate ion is an essential component of biological systems and is vital to many cellular processes in mammals, such as intracellular pH homeostasis, kidney function and sperm maturation. However, very little is known about how HCO_3^- fluctuates within a cell in response to cell stimuli and methodology for such analysis is limited to gross measurement of $H^{14}CO_3^-$ uptake and inferences based upon changes in intracellular pH. Knowledge about how HCO_3^- is localised and varies within a compartment is essential for our understanding of the diverse physiological processes it may control *e.g.* cyclic–AMP regulation, through reversible binding to a soluble adenylyl cyclase enzyme.[42] Moreover, the pathological consequences of the perturbation of some of these physiological processes are likely to be profound: mis-expression of carbonic anhydrase (CA) is associated with a variety of tumour types and CAII deficiency syndrome in humans is characterised by renal tubular acidosis, osteoporosis and mental retardation. Evidently, there is a need for a direct method for assaying changes in HCO_3^- concentration within a cell, and to follow the changes in different compartments (*e.g.* mitochondria) in real time.

A series of europium–acridone conjugates has been reported[31] that reveal a 300% change in the intensity ratio of the 618/588 nm emission bonds in the physiologically relevant bicarbonate concentration range, 5 to 25 mM in the presence of competing anions and protein. Affinity for the anion has been controlled by varying the peripheral electrostatic gradient in these complexes and anionic, zwitterionic and overall cationic complexes have been examined that retain the desired selectivity for bicarbonate. The complexes are non-toxic to cells ($\leq$ 5 mM), and the imaging of cells by confocal microscopy reveals uptake and clear intracellular staining that is dependent upon anion binding to the Eu centre. Such work augurs well for the application of these probes to image intracellular HCO_3^- fluctuations, and hence enhance our understanding of the biological significance of the pre-eminent C_1 oxyanion.

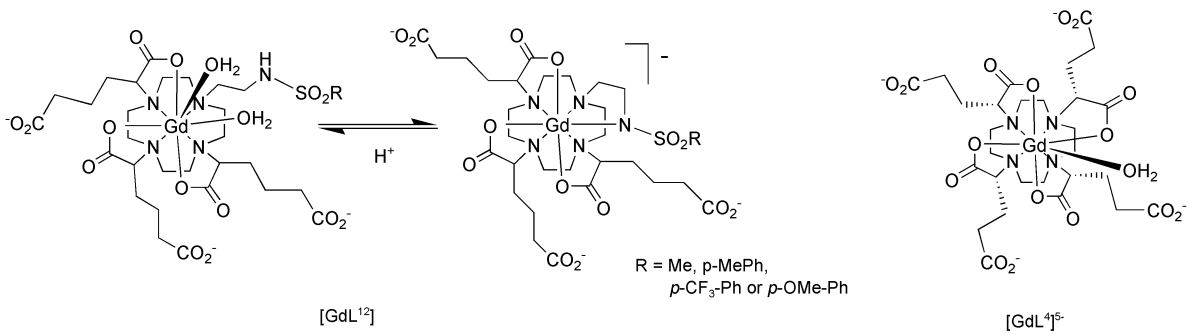

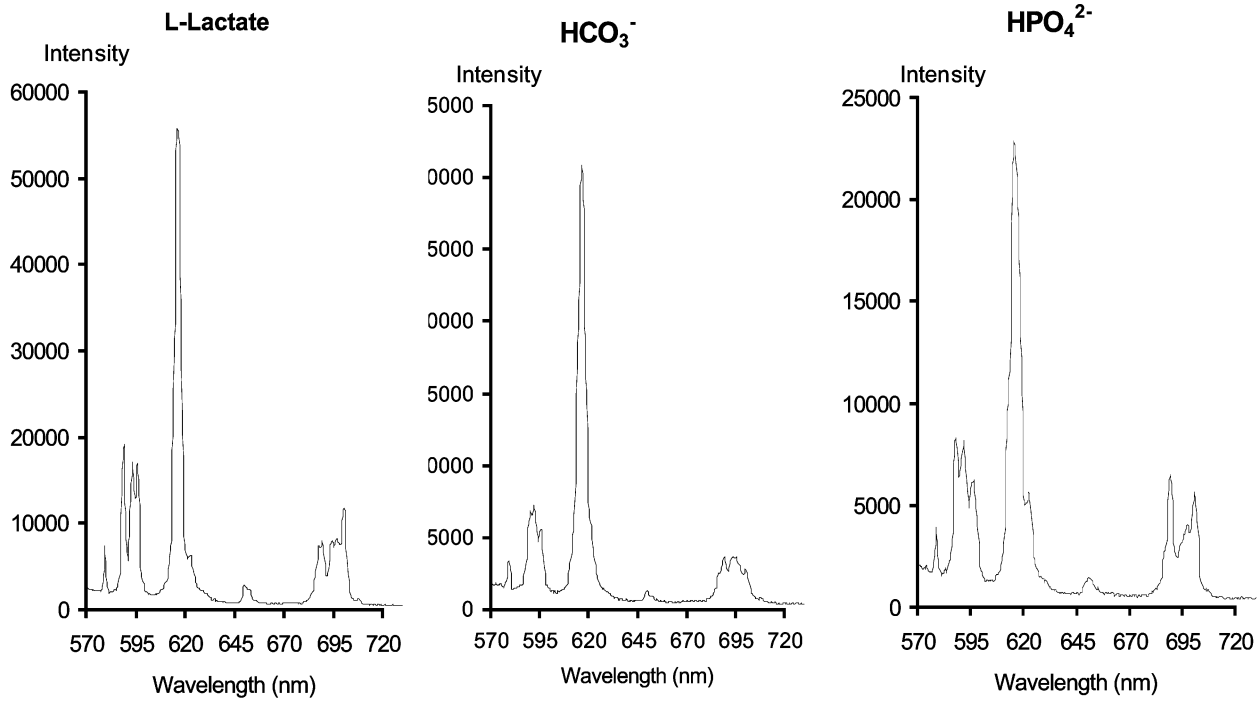

Fig. 11 Europium emission spectra for (EuL[13]] (0.1 mM, l mM anion, pH 7.4, λ_{exc} 410 nm) in the presence of excess (*S*)-lactate (left), bicarbonate (centre) and hydrogenphosphate, revealing the changes in spectral form accompanying reversible anion coordination.

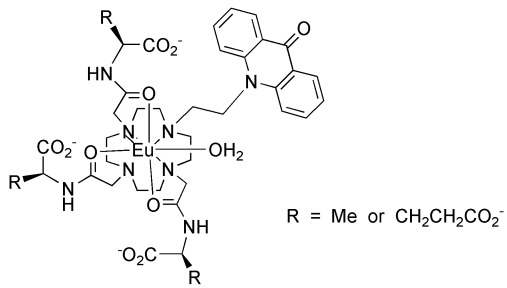

[EuL[13]]

5.2 Conclusions

There are several important issues which have become clearer as a consequence of the recent surge of activity in studying well-defined lanthanide complexes. In 9-coordinate complexes adopting tri-capped trigonal prismatic and monocapped square antiprismatic geometries, a water molecule adopting a capping site is sitting in a sterically demanding site. Such a site, being destabilised by steric compression, leads to a weakening of the Ln–water bond and is accompanied by a strengthening of the H-bonding interaction between the bound water oxygen and the nearest second sphere water protons, leading to an enhanced rate of dissociative water exchange. In complexes approximating to axial symmetry, the ligand sitting on the principal axis plays a key role in determining the ligand field. It is the polarisability of the ligand donor that determines the local magnetic susceptibility anisotropy, expressed in both shifted NMR spectra and in the form of absorption/circular dichroism, and emission/circularly polarised luminescence spectra: this is most apparent for Eu and Yb complexes but is a general effect across the series. Such work is aiding analysis of variations in spectral profiles that characterise the behaviour of new series of responsive lanthanide probes, tailored to act as MR, MRI or luminescent probes that are poised to extend the current feeling of excitement in lanthanide chemistry research, and perhaps sustain the relevance of undergraduate lectures on this topic!

Acknowledgements

The author is indebted to the inspiration and graft of his co-workers and collaborators in Durham, Glasgow (Bob Peacock), Duluth (Jim Riehl) and Torino (Mauro Botta and Silvio Aime) without whom none of this work would have been achieved. Intermittent financial support from EPSRC, BBSRC EC/ESF COST-D-18 and the Royal Society is also humbly acknowledged.

References

1 Frontiers in Lanthanide Chemistry, *Chem. Rev.*,2002, **102**, (6)), 1807–2476.
2 *Metal Ions in Biological Systems*: *The Lanthanides and their Interrelations with Biosystems*, **Vol. 40,** eds., H. Sigel and A. Sigel, Marcel Dekker, Basel, 2003.
3 C. C. Hinckley, *J. Am. Chem. Soc.*, 1969, **91**, 5160; G. M. Whitesides and D. W. Lewis, *J. Am. Chem. Soc.*, 1970, **92**, 6979; R. R. Fraser, M. A. Petit and J. K. Saunders, *J. Chem. Soc., Chem. Commun.*, 1971, 1450; J. Reuben and D. Fiat, *J. Chem. Soc., Chem. Commun.*, 1967, 729; K. Kabuto and Y. Sasaki, *J. Chem. Soc., Chem. Commun.*, 1984, 316; J. Reuben, *J. Am. Chem. Soc.*, 1980, **102**, 2232.
4 K. G. Morallee, E. Niebser, F. J. C. Rossotti, R. J. P. Williams and A. V. Xavier, *J. Chem. Soc., Chem. Commun.*, 1970, 1132.
5 C. F. G. C. Geraldes and C. Luchinat, in *Metal Ions in Biological Systems: The Lanthanides and their Interrelations with Biosystems*, eds. H. Sigel and A. Sigel, Marcel Dekker, NewYork, chapter 14, 2003, 514–588.
6 *The Chemistry of Contrast Agents for Medical Magnetic Resonance Imaging*, eds. A. E. Merbach and E. Toth, Wiley, London, 2001.
7 C. D. Barry, A. C. T. North, J. A. Glasel, R. J. P. Williams and A. V. Xavier, *Nature*, 1971, **232**, 236.
8 D. Bentrap, I. Bertini, M. A. Cremonini, S. Forsén, C. Luchinat and A. Malmendal, *Biochemistry*, 1997, **36**, 13629.
9 P. K.-L. Fu and C. J. Turro, *J. Am. Chem. Soc.*, 1999, **121**, 1; S. L. Klakamp and W. D. Horrocks, *Biopolymers*, 1990, **30**, 33.
10 W. De W. Horrocks and D. R. Sudnick, *J. Am. Chem. Soc.*, 1979, **101**, 334.
11 D. Parker and J. A. G. Williams in *Metal Ions in Biological Systems: The Lanthanides and their Interrelations with Biosystems*, eds. H. Sigel and A. Sigel, Marcel Dekker, New York, chapter 7, 2003, 233–280.
12 R. S. Dickins, D. Parker, H. Puschmann, C. Crossland and J. A. K. Howard, *Chem. Rev.*, 2002, **102**, 1977.For details of Ln–OH_2 variations

in a related tripodal neutral complex see: Y. Bretonniere, M Mazzanti, J. Pecaut, F. Dunand and A. E. Merbach, *Inorg. Chem.*, 2001, **40**, 6737.
13 D. Parker, H. Puschmann, A. S. Batsanov and K. Senanayake, *Inorg. Chem.*, 2003, **42**, 8646.
14 F. A. Dunand, R. S. Dickins, A. E. Merbach and D. Parker, *Chem. Eur. J.*, 2001, **7**, 5160; S. Zhang, K. Wu and A. D. Sherry, *J. Am. Chem. Soc.*, 2002, **124**, 4226.
15 S. Aime, A. Barge, A. S. Batsanov, M. Botta, D. D. Castelli, F. Fedeli, A. Mortillaro, D. Parker and H. Puschmann, *Chem. Commun.*, 2002, 1120.
16 P. Caravan, J. J. Ellison, T. J. McMurry and R. B. Lauffer, *Chem. Rev.*, 1999, **99**, 2293.
17 M. Botta, *Eur. J. Inorg. Chem.*, 2000, 399.
18 M. Woods, S. Aime, M. Botta, J. A. K. Howard, J. M. Moloney, M. Navet, D. Parker. M. Port and O. Rousseaux, *J. Am. Chem. Soc.*, 2000, **122**, 9781.
19 G. Muller, S. D. Kean, D. Parker and J. P. Riehl, *J. Phys. Chem. A*, 2002, **106**, 12349.
20 A. Beeby, I. M. Clarkson, R. S. Dickins, S. Faulkner, D. Parker, L. Royle, A. S. de Sousa, J. A. G. Williams and M. Woods, *J. Chem. Soc., Perkin Trans. 2*, 1999, 493.
21 P. Hermann, I. Lukes private communication.
22 S. Aime, M. Botta, D. Parker and J. A. G. Williams, *J. Chem. Soc., Dalton Trans.*, 1996, 17.
23 E. Terreno, S. Aime, A. Barge, D. D. Castelli and F. U. Nielsen, *J. Inorg. Biochem.*, 2001, **86**, 41; S. R. Zhang, P. Winter, K. C. Wu and A. D. Sherry, *J. Am. Chem. Soc.*, 2001, **123**, 1517.
24 M. Eigen, *Pure Appl. Chem.*, 1963, **6**, 105; R. G. Wilkins and M. Eigen, *Adv. Chem. Ser.*, 1965, **49**, 55; D. W. Margerum in *Coordination Chemistry* ed. A. E. Martell, ACS Monograph, ACS, Washington 1978, **vol. 174**, chapter 1.
25 D. T. Richens, *The Chemistry of Aqua Ions*, Wiley, Chichester, 1997.
26 B. Hribar, N. T. Southall, V. Vlacky and K. R. Dill, *J. Am. Chem. Soc.*, 2002, **124**, 12302.
27 K. D. Collins, *Biophys. J.*, 1997, **72**, 65.
28 A. Barge, M. Botta, D. Parker and H. Puschmann, *Chem. Commun.*, 2003, 1386.
29 G. Bobba, J.-C. Frias and D. Parker, *Chem. Commun.*, 2002, 890. See also: B. H. Bakker, M. Goes, N. Hoebe, H. J. van Ramesdonk J. W. Verhoeven, M. H. V. Werts and J. W. Hofstraat, *Coord. Chem. Rev.*, 2000, **208**, 3.
30 A. Dadabhoy, S. Faulkner and P. G. Sammes, *J. Chem. Soc., Perkin Trans. 2*, 2000, 2359; A. Beeby, L. M. Bushby, D. Maffeo and J. A. G. Williams, *J. Chem. Soc., Perkin Trans. 2*, 2000, 1281.
31 Y. Brettoniere, M. J. Cann, D. Parker and R. Slater, *Chem. Commun.*, 2002, 1930.
32 D. Parker, *Coord. Chem. Rev.*, 2000, **205**, 109.
33 D. Parker, P. K. Senanayake and J. A. G. Williams, *J. Chem. Soc., Perkin Trans. 2*, 1998, 2129.
34 S. Blair, R. Kataky and D. Parker, *New J. Chem.*, 2002, **26**, 530.
35 M. P. Lowe, D. Parker, O. Reany, S. Aime, M. Botta, G. Castellano, E. Gianolio and R. Pagliarin, *J. Am. Chem. Soc.*, 2001, **123**, 7601.
36 J. I. Bruce, R. S. Dickins, L. J. Govenlock, T. Gunnlaugsson, S. Lopinski, M. P. Lowe, D. Parker, R. D. Peacock, J. J. B. Perry, S. Aime and M. Botta, *J. Am. Chem. Soc.*, 2000, **122**, 9674.
37 B. Bleaney, *J. Magn. Reson.*, 1972, **8**, 91.
38 L. DiBari, G. Pintacuda, P. Salvadori, R. S. Dickins and D. Parker, *J. Am. Chem. Soc.*, 2000, **122**, 9257.
39 R. S. Dickins, D. Parker, J. I. Bruce and D. J. Tozer, *J. Chem. Soc., Dalton Trans.*, 2003, 1264.
40 W.-H. Li, S. E. Fraser and T. J. Meade, *J. Am. Chem. Soc.*, 1999, **121**, 1431.
41 R. S. Dickins, S. Aime, A. S. Batsanov, A. Beeby, M. Botta, J. I. Bruce, J. A. K. Howard, C. S. Love, D. Parker, R. D. Peacock and H. Puschmann, *J. Am. Chem. Soc.*, 2002, **124**, 12697; R. S. Dickins, A. S. Batsanov, J. A. K. Howard, D. Parker, H. Puschmann and S. Salamano, *Dalton Trans.*, 2004, 70.
42 Y. Chen, M. J. Cann, T. N. Litvin, V. Iourgenko, M. L. Sinclair, L. R. Letvin and J. Buck, *Science*, 2000, **289**, 625.